SWIFT XRT CALDB RELEASE NOTE
SWIFT-XRT-CALDB-09: Response matrices and Ancillary Response Files

1. Component Files:

Filename	Mode	Grade	Date
swxwt0to2_20010101v009.rmf	WT	0-2	04/27/07
swxwt0to2_20010101v009.arf			
swxwt0_20010101v009.rmf	WT	0	04/27/07
swxwt0_20010101v009.arf			
swxpc0to12_20010101v009.rmf	PC	0-12	04/27/07
swxpc0to12_20010101v009.arf			
swxpc0_20010101v009.rmf	PC	0	04/27/07
swxpc0_20010101v009.arf			
swxpd0to5_20010101v009.rmf	*LRPD*	*0-5*	*07/04/2005*
swxpd0to5_20010101v009.arf			*04/05/2005*
swxpd0to2_20010101v009.rmf	*LRPD*	*0-2*	*07/04/2005*
swxpd0to2_20010101v009.arf			*04/05/2005*
swxpd0_20010101v009.rmf	*LRPD*	*0*	*07/04/2005*
swxpd0_20010101v009.arf			*04/05/2005*

2. Scope of Document

This note describes the release of the Swift XRT redistribution matrix (RMF v9) and ancillary response (ARF v9) files. Files are released for each working XRT mode (Photon Counting, PC, Window Timing, WT) and two different grade selections for each mode[1]. The XRT effective area is made by three main components: the mirror effective area, the CCD quantum efficiency (QE) and the filter transmission. The QE is included directly in the redistribution matrix. The ARF files contain the mirror effective area, the filter transmission, as well as the vignetting correction and the Point Spread Function (PSF) correction (which depends on the source location and of the size of the extraction region, as well as on defects on the CCD).

Here we report on the CALDB RMF and ARF files which represent the effective area of the telescope for a nominal on-axis observation (no vignetting correction) and for an infinite region of interest (no correction for PSF losses). RMF files do not include the PSF correction and do not depend on the source position on the detector. The CCD soft energy response is sufficiently uniform within the central 200x200 pixels (see e.g. previous RMF release notes), therefore there is just one RMF file per mode and grade selection. The ARF files, instead, need vignetting and PSF corrections and, therefore, need to be built for each observation. To produce the observation-specific ARF files, the *xrtmkarf* task (XRTDAS-HEADAS software) has been developed. This task corrects the nominal ARF file for the vignetting and, optionally (psfflag=yes), for PSF losses. This task includes corrections for CCD defects with the inclusion of an exposure map automatically generated by the data analysis pipeline (expofile=filename.img). The adopted calibration method implies that we include the residual correction of the CCD quantum efficiency in the CALDB ARF files. This explains why the nominal ARF files are different for different grade selection.

3. RMF generation

The Response Matrix Files (RMFs) are created by a Monte-Carlo simulation code (Osborne et al. 2005, SPIE 5859 340). This code models: transmission of the incident X-rays through the CCD electrode structure; photo-absorption in the active layers of the device; charge cloud generation, transportation and spreading; silicon fluorescence and its associated escape peak; surface loss effects; mapping of the resultant charge-cloud to the detector pixel array; charge transfer efficiency; addition of electronic read-out noise; event thresholding and classification according to the specific mode of operation.
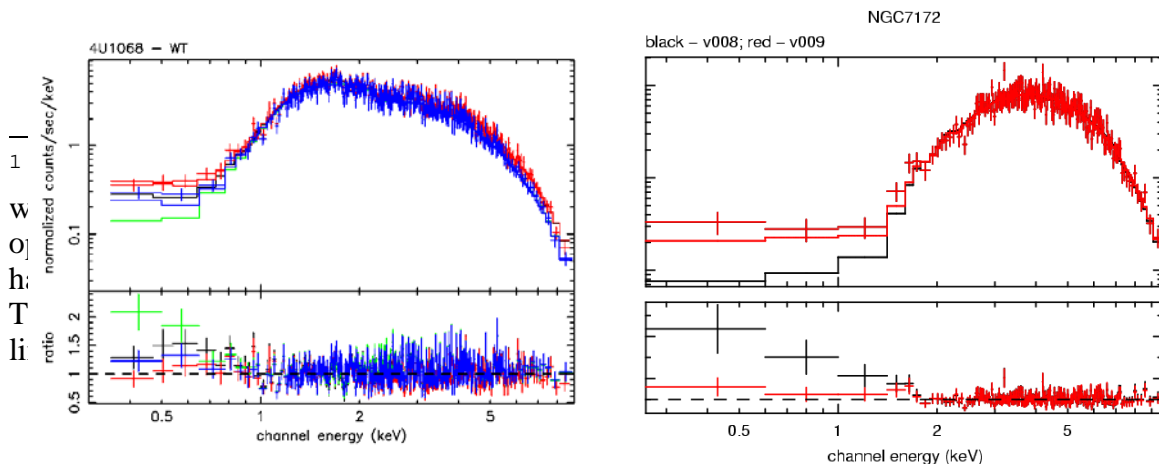
Figure 1: Left - Fits to 4U1608-52 in WT mode showing the improvement obtained with the v009 RMF to absorbed sources (v009: red grade 0-2, blue grade 0 – v008: black grade 0-2, green grade 0. Right - similarly for the absorbed source NCG7172 in PC mode (v009: red grade 0-12 – v008: black grade 0-12).

Specifically, for this release, in orbit observations of the soft calibration sources were used to refine the surface loss function in order to better match the spectral redistribution at low energies. While for heavily absorbed sources, the parameterisation of the redistribution of high energy X-rays down to low energies was improved for both PC and WT modes (using SNR G21.5 & SGR 1900+14 for PC, and GROJ1655-40, 4U1608-52 and GX17+2 for WT) by including a correction to the loss-shelf (see figure 1). For PC mode, a new charge-cloud spreading model was implemented following the theory of Pavlov & Nousek (1999 NIMA 428 348), which better accounts for sub-threshold losses seen in the more energetic multi-pixel events. For both modes, updated Charge Transfer Inefficiency (CTI) values were used, which are more appropriate for the CTI degradation suffered in orbit.

4. ARF generation

In order to model the overall XRT response we used the latest RMF matrices (hereby released) and fine tuned the ARF files on X-ray spectra from different celestial sources. Following the previous release, we adopted a multi-source approach, with the sources having different spectral characteristics, to improve the calibration. We did this by comparing the spectral parameters and absolute flux of several calibration sources with spectra taken by XMM-Newton (primarily the EPIC-MOS) in order to improve the absolute flux determination in both WT and PC modes, as well as use the same source in WT and PC, wherever possible, to ensure consistency between the two.

4.1 Windowed Timing Mode

First of all, we become fully aware that the off-pulse spectrum of the Crab nebula is still slightly piled-up, so to improve the XRT response description we did not use this source to calibrate the WT mode. Another step forward came with the opportunity to dynamically correct for possible bias offsets in WT mode observations within *xrtpipeline* using the *wtbiasmode=M20P* option (which, since build 2.6 of the Swift software tools, is now the default). This option computes the bias difference between the on-ground estimated bias median from the last 20 pixels data telemetered with every frame, and the median of the last 20 pixels in the related bias row (which was subtracted automatically on-board).[2] This improved, substantially, the description of the WT mode data and led us to be confident in the reality of the absorption-like feature observed in a number of spectra at low energies. We thus corrected for this feature in the effective area of WT (and PC) mode.

The first improvement to the ARF at low energies came by including the detailed

---

[2]   Note, a similar option for PC mode, based on the corner pixels of single-pixel events will be implemented in the next (May 2007) XRT software release.

medium-thickness filter transmission curve from the XMM-Newton MOS detector. This is identical in composition and thickness to the Swift XRT filter, so that differences between the two are expected to be negligible. This new filter curve introduces a number of fine structure features in the O-edge (0.54 keV) and Al-edge (1.56 keV).

We then used as a primary calibrator for WT mode two observations of Mkn 421. The first (obsid 00030352011, 33ks exposure with 1.3e6 counts) was used to apply ad-hoc corrections to residuals around the Au edges (2.2-3.0 keV), near the O-edge (0.52 keV), the Si-edge (1.84 keV), and a further residual at 0.93 keV. The second observation (obsid 00030352017, 4.4ks exposure), which was taken simultaneously with the XMM-Newton EPIC cameras (in timing mode), was used to verify that the derived spectral fit parameters were acceptable. Fitting an absorbed, continuously bending power-law model to these data we obtained:

	Photon Index	Bending Parameter	Flux (0.3-10.0 keV) (erg cm^{-2} s^{-1})
MOS1	2.365±0.015	-0.42±0.03	4.48e-10
WT g0-2	2.395±0.018	-0.36±0.03	4.29e-10

Additionally, observations of the quasar 3c273 (obsid 00050900010/1), taken simultaneously with XMM, were compared in order to verify the global effective area and spectral parameters (modelled by an absorbed power-law plus black-body):

	Photon Index	Blackbody Temp (keV)	Flux (0.3-10.0 keV) (ergs cm^{-2} s^{-1})
PN	1.486±0.003	0.110±0.002	1.85e-10
MOS1/2	1.456±0.004	0.071±0.004	1.96e-10
WT g0-2	1.466±0.019	0.088±0.007	2.05e-10

The above results show that the XRT WT grade 0-2 flux is accurate to 5% compared with the MOS. Note, also, the WT grade 0-2 and grade 0 fluxes are comparable to each other to within a few per cent.
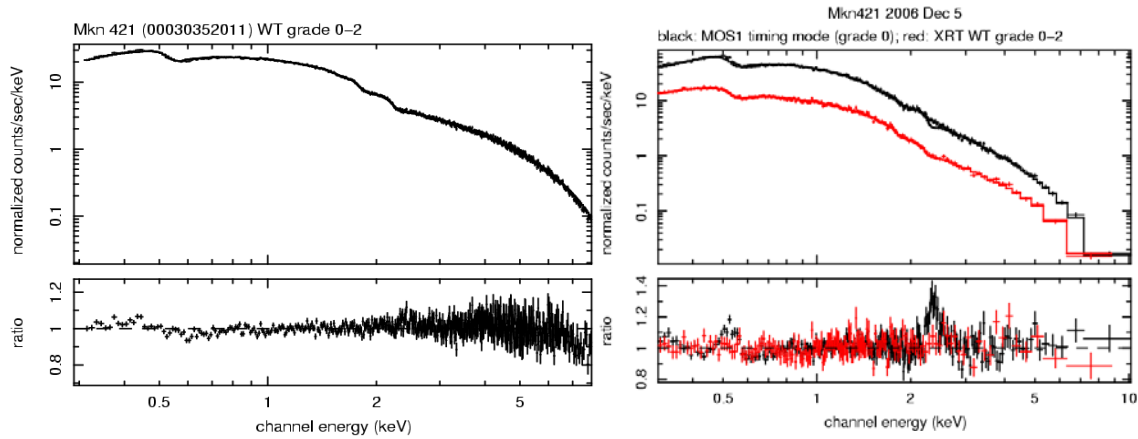

Figure 2: Left – the high S/N WT dataset of Mkn421 which was used to fine tune the residuals around the Au, Si, and O edges, fitted with the v009 calibration. Right – a comparison of the simultaneous MOS1 timing mode data (black, the large residuals are due to uncorrected response around the gold-edge) and XRT WT data (red) from 2006

Dec 5 which was used to verify the spectral parameters.

An observation of the isolated neutron star RXJ1856-37 was used to normalise the effective area at low energies (< 0.8 keV). Using the model of Beuermann et al. (2006 A&A 458 541, derived from Chandra LETG), which is essentially a 63 eV black-body in the XRT band, we find that the soft band flux is also accurate to approximately 5%.
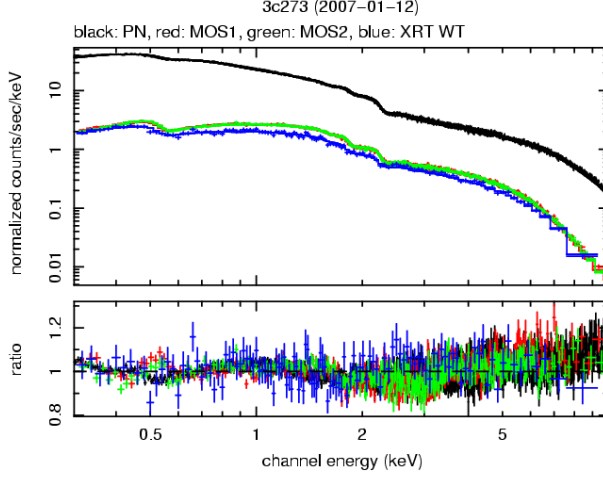

Figure 3: Simultaneous XMM-Newton and Swift observations of 3c273 showing the PN (black), MOS1 (red), MOS2 (green), and XRT WT mode (blue) fit and residuals.

In conclusion, we recommend to fit XRT WT spectra in the 0.3-10 keV energy range with these updated XRT response files. A systematic less than 3% is needed for very bright sources.

4.2 Photon Counting mode

In PC mode, the ARF files were calibrated on the stable Crab-like plerion PSR B0540-69, with parameters determined from a deeper XMM-Newton observation. Fitting a model consisting of TBabs*(powerlaw + vnei), with the temperature and abundances of the latter component fixed, gives:

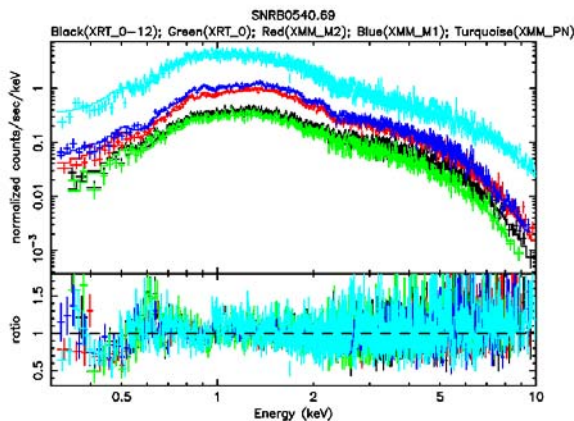|	N_H (10^{22} cm^2)	Photon Index	Flux (0.3-10 keV) (ergs cm^{-2} s^{-1})
PN	0.57±0.02	2.01±0.02	3.26e-11
MOS1	0.58±0.02	2.06±0.03	3.96e-11
MOS2	0.53±0.02	2.05±0.03	3.72e-11
PC g0-12	0.48±0.02	2.01±0.03	3.78e-11
PC g0	0.49±0.02	2.04±0.04	3.68e-11

Figure 4: Comparison of the Swift XRT PC mode observation (grade 0-12, black; grade 0, green) of PSR B0540-69 with XMM (PN, cyan; MOS1, blue; MOS2, red).

The strongest features in the PSR 0540-69 spectrum are an absorption feature at ~0.45 keV and an emission feature at slightly higher energies. This feature is large and might be related to the source itself as the XMM-Newton spectra show a similar residual. The PC mode and EPIC MOS fluxes are consistent to within 8%.

As with WT mode, the soft neutron stars RXJ1856-37 and RXJ0720-31 were used to validate the PC mode effective area at low energies, showing consistency better than 6% below 0.5 keV. In addition to this, observations a number of other sources, such as SNR G21.5, and the cluster of galaxies PKS0745-19, were considered.

The statistical uncertainty on the final RMF+ARF matrices in PC mode is estimated at 3% level in the 0.3-10 keV energy range.
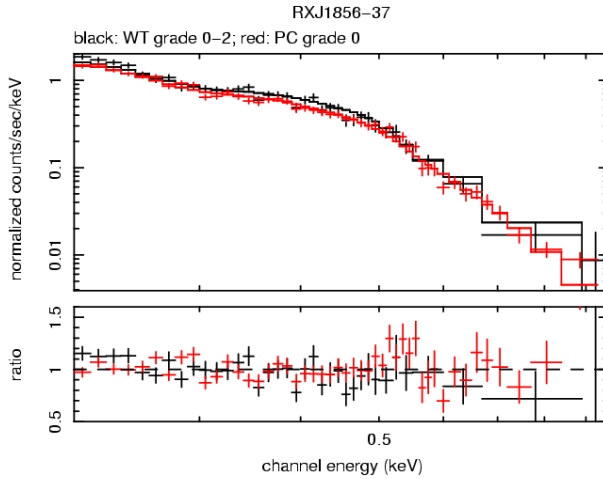

Figure 5: WT grade 0-2 and PC grade 0 spectra of the soft neutron star RXJ1856-37 modelled with an absorbed black-body.

5. Current limitations and future prospects

Our current understanding of the XRT response still implies a systematic uncertainty of the order of 2.5% in the 0.3-10 keV energy band (the recommended band to be used) and better than 10% in absolute flux. The following considerations apply to both WT and PC mode observations.

● While the loss-shelf has been improved, and with it the modelling of the redistribution for heavily absorbed sources, there is still scope for future enhancements in this area.
● We are starting observing a degradation of the charge transfer inefficiency (CTI), from 80 eV FWHM to 105 eV FWHM at 1.8 keV (based on Cas A spectra). Time dependent response matrices will have to be developed in the future.
● We discovered the presence of charge traps in the CCD. These will generate small energy scale problems at low energies (possibly in relation to bright Earth contamination). Prospects to implement a column by column description of the bias correction are under investigation.